Factors Governing Intrinsic Chemical Reactivity Differences between Clavulanic and Penicillanic Acids

Yen-lin Lin,[†] Nai-yuan Chang,[‡,§] and Carmay Lim*,[†,‡]

Contribution from the Department of Chemistry, National Tsing Hua University, Hsinchu 300, Taiwan, R.O.C., and Institute of Biomedical Sciences, Academia Sinica, Taipei 11529, Taiwan, R.O.C.
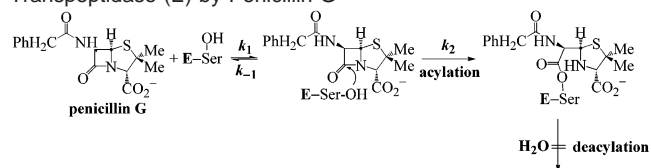
Abstract: To help elucidate why penicillin-G is inactivated by certain bacterial β-lactamase enzymes, whereas clavulanic acid (Clav, which is similar to penicillin-G except at positions 1, 2, and 6) inhibits β-lactamase, the intrinsic chemical reactivities of these two antibiotics were assessed in this work. Ab initio and continuum dielectric methods were used to map out the gas-phase and solution-phase free-energy profiles for the alkaline hydrolyses of Clav and penicillanic acid (Peni, which is similar to penicillin-G except at position 6) as well as of a fictitious hybrid compound, Peni-db, which is similar to Clav and Peni except at positions 1 and 2, respectively. Furthermore, the ring strain energies of various lactam rings and the five-membered rings of Peni and Clav as well as their respective rate-limiting transition states were computed to assess the contribution of four- and five-membered ring strains to the antibiotic's activity. The predicted product distribution, rate-limiting step, and relative reaction rates for the alkaline hydrolysis of Peni and Clav are in accord with the experimental findings. The rate-limiting step in the alkaline hydrolysis of Peni, Clav, or Peni-db is the approach of the negatively charged hydroxide ion toward the anionic reactant to form a tetrahedral intermediate. The alkaline hydrolysis of Clav generates more stable products than that of Peni mainly because the O1 atom and the hydroxyethylidene group in Clav facilitate the opening of the five-membered ring; furthermore, the O1 atom can abstract a proton easier than the less polar S1 in Peni. Clav undergoes basic hydrolysis faster than Peni mainly because its hydroxyethylidene group leads to an increase in the positive charge on the carbonyl C7 atom, therefore enhancing favorable electrostatic interactions with the incoming hydroxide anion. To a lesser extent, the oxygen at position 1 in Clav also contributes to the rate acceleration because of the greater solvent stabilization of the oxygen-containing transition state as compared to the respective ground state. The inherent strain of the four-membered β-lactam ring or five-membered ring does *not* enhance the alkaline hydrolyses of β-lactam molecules such as Peni or Clav, consistent with the observation that the rate-limiting step does not involve a breakdown of the four-membered β-lactam ring or five-membered thiazolidine/oxazolidine rings.

Introduction

β-lactam antibiotics, like penicillins, cephalosporins, thienamycins, and related antimicrobial agents,[1-6] have been effective drugs for fighting various bacterial infections. They have in
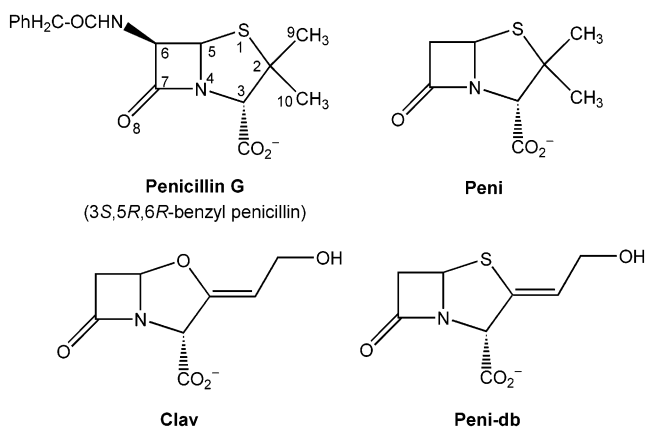
* To whom all correspondence should be addressed: Carmay Lim, Institute of Biomedical Sciences, Academia Sinica, 11529 Taipei, Taiwan. E-mail: carmay@gate.sinica.edu.tw. Phone: 886-2-2652-3031. Fax: 886-2-2788-7641.
† National Tsing Hua University.
‡ Academia Sinica.
§ Current address: Department of Chemistry, Massachusetts Institute of Technology, Cambridge, MA 02139.

(1) Buynak, J. D.; Khasnis, D.; Bachmann, B.; Wu, K. C.; Lamb, G. *J. Am. Chem. Soc.* **1994**, *116*, 10955–10965.
(2) Bulychev, A.; Obrien, M. E.; Massova, I.; Teng, M.; Gibson, T. A.; Miller, M. J.; Mobashery, S. *J. Am. Chem. Soc.* **1995**, *117*, 5938–5943.
(3) Jackson, P. M.; Roberts, S. M.; Davalli, S.; Donati, D.; Marchioro, C.; Perboni, A.; Proviera, S.; Rossi, T. *J. Chem. Soc., Perkin Trans. 1* **1996**, 2029–2039.
(4) Ghosh, A.; Ghosh, M.; Niu, C.; Malouin, F.; Moellmann, U.; Miller, M. J. *Chem. Biol.* **1996**, *3*, 1011–1019.
(5) Wladkowski, B. D.; Chenoweth, S. A.; Sanders, J. N.; Krauss, M.; Stevens, W. J. *J. Am. Chem. Soc.* **1997**, *119*, 6423–6431.
(6) Nangia, A.; Chandrakala, P. S.; Balaramakrishna, M. V.; Latha, T. V. A. *THEOCHEM* **1995**, *343*, 157–165.

common a β-lactam ring fused to a five- or six-membered heteroring to form a bicyclic molecule with a rigid V-shape conformation. β-lactam antibiotics are thought to mimic the structures of the C-terminal *D*-alanyl-*D*-alanine residues of the peptide chain of uncross-linked peptidoglycan.[7] They inhibit transpeptidase, an enzyme involved in forming the bacterial cell wall, by acylating its active site serine irreversibly to form an acyl-enzyme intermediate (see Scheme 1). Consequently, the transpeptidase cannot catalyze the last step of bacterial cell-wall biosynthesis, resulting in cell death.

Scheme 1. Schematic Diagram Showing the Inhibition of Transpeptidase (E) by Penicillin-G

However, some β-lactam antibiotics are no longer effective against certain strains of bacteria; for example, penicillin-G

Figure 1. Schematic diagram of penicillin-G, Clav, Peni, and Peni-db. Penicillin G is also known as 3S,5R,6R-benzyl penicillin.

(Figure 1) is no longer effective against *Staphylococcus aureus* FAR10.[8–10] This is because bacteria have evolved an effective defense mechanism against some antibiotics by producing β-lactamase. Most β-lactamases (Classes A, C, and D) are serine proteases,[11] which degrade β-lactam antibiotics as shown in Scheme 2. The active site serine hydroxyl group attacks the β-lactam sp[2] carbonyl carbon to form an acyl-enzyme intermediate that subsequently undergoes deacylation to generate the enzyme and the degraded antibiotic. Therefore, β-lactam antibiotics become futile if the β-lactamase enzyme hydrolyzes them before they reach the transpeptidase.[12]
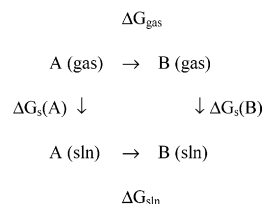
Fortunately, other antibiotics that can inactivate β-lactamases from a variety of gram-positive and gram-negative bacteria have been found. One such example is clavulanic acid (Clav),[13] which was isolated from *Streptomyces clavuligerus* in 1976.[14] As shown in Figure 1, Clav is similar to penicillin-G except at three moieties: at position 1, an oxygen replaces a sulfur; at position 2, a hydroxyethylidene group replaces two methyl groups; and at position 6, there is no substituent. Unlike penicillin-G, which is inhibited by β-lactamase, Clav inhibits β-lactamase and, to a lesser extent, transpeptidase.[15] The proposed mechanism of β-lactamase inhibition by Clav[12,15–20] depicted in Scheme 3 is similar to that of transpeptidase inhibition by penicillin-G in Scheme 1 in that Clav, like penicillin-G, inhibits the enzyme by acylating its active site serine irreversibly to form an acyl-enzyme intermediate. However, unlike penicillin-G, the initial acyl-enzyme intermediate can rearrange into a chemically inert enamine, whose further reaction the enzyme is unable to catalyse.

(7) Tipper, D. J.; Strom
inger, J. L. *Proc. Natl. Acad. Sci. U.S.A.* **1965**, *54*, 1133–1141.
(8) East, A. K.; Dyke, K. G. H. *J. Gen. Microbiol.* **1989**, *135*, 1001–1015.
(9) Zygmunt, D. J.; Stratton, C. W.; Kernodle, D. S. *Antimicrob. Agents Chemother.* **1992**, *36*, 440–445.
(10) Bonfiglio, G.; Livermore, D. M. *J. Antimicrob. Chemother.* **1994**, *33*, 465–481.
(11) Page, M. I. *Adv. Phys. Org. Chem.* **1987**, *23*, 165–270.
(12) Knowles, J. R. *Acc. Chem. Res.* **1985**, *18*, 97–104.
(13) Howarth, T. T.; Brown, A. G.; King, T. J. *J. Chem. Soc., Chem. Commun.* **1976**, 266–267.
(14) Brown, A. G.; Butterworth, D.; Cole, M.; Hanscomb, G.; Hood, J. D.; Reading, C.; Rolinson, G. N. *J. Antibiot.* **1976**, *29*, 668–669.
(15) Reading, C.; Cole, M. *Antimicrob. Agents Chemother.* **1977**, *11*, 852–857.
(16) Brenner, D. G.; Knowles, J. R. *Biochemistry* **1984**, *23*, 5833–5839.
(17) Fisher, J.; Charnas, R. L.; Knowles, J. R. *Biochemistry* **1978**, *17*, 2180–2184.
(18) Charnas, R. L.; Fisher, J.; Knowles, J. R. *Biochemistry* **1978**, *17*, 2185–2189.
(19) Charnas, R. L.; Knowles, J. R. *Biochemistry* **1981**, *20*, 3214–3219.
(20) Cartwright, S. J.; Coulson, A. F. *Nature (London)* **1979**, *278*, 360–361.

Here, to help elucidate why Clav, which is similar to penicillin-G, can inhibit β-lactamase, while penicillin-G cannot, the intrinsic chemical reactivities of the two antibiotics were assessed. To this end, we mapped out the free-energy profiles for the alkaline hydrolyses of Clav and penicillanic acid (Peni in Figure 1 whose structure is similar to that of penicillin-G except that there is no substituent at position 6). These two molecules were chosen for study because their second-order rate constants for alkaline hydrolysis at 303.15 K have been measured and can, thus, be compared with the calculated values. A fictitious compound, referred to as Peni-db (Figure 1), which differs from Clav only at position 1 and from Peni only at position 2, was also studied to investigate the chemical reactivity difference between Peni and Clav.

To evaluate the hypothesis that the antibiotic's activity is due to the inherent strain of the four-membered β-lactam ring,[21] ring strain energies[22] of various lactam rings were computed. In addition, the ring strain energies of the five-membered rings of Peni and Clav, their respective rate-limiting transition states, and tetrahedral intermediates were also calculated. The free-energy profiles for the alkaline hydrolyses of Peni, Clav, and Peni-db were mapped out, as outlined in the next section. The predicted product distribution, rate-limiting step, and reaction rates for the alkaline hydrolyses of Peni and Clav were compared to those found experimentally to verify the reliability of the calculations. The results of the calculations reveal the factors governing the different products observed in the alkaline hydrolyses of Peni and Clav as well as the factors governing the enhanced reactivity of Clav relative to Peni. The approach, validation steps, and analyses presented in this work could also be applied to elucidate the differences in the "*intrinsic chemical*" reactivities of similar substrates, which is an important first step before conclusions can be made about the effect of the substituents on enzyme recognition/function.

Methods

Solution Free-Energy Barrier. The free-energy barrier in solution, ΔG_{sln}, from A to B was calculated from the following thermodynamic cycle:
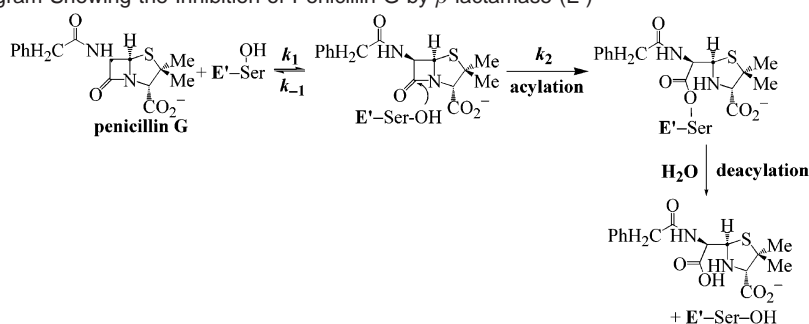
$$
\begin{array}{ccc}
& \Delta G_{gas} & \\
A\ (gas) & \rightarrow & B\ (gas) \\
\Delta G_s(A) \downarrow & & \downarrow \Delta G_s(B) \\
A\ (sln) & \rightarrow & B\ (sln) \\
& \Delta G_{sln} &
\end{array}
$$

ΔG_{gas}, the gas-phase free-energy barrier, was obtained by ab initio calculations, whereas ΔG_s, the solvation free energy, was estimated by solving Poisson equation using finite difference methods (see below). Thus, the solution free-energy barrier from A to B was computed from

$$\Delta G_{sln} = \Delta G_{gas} + \Delta G_s(B) - \Delta G_s(A) \qquad (1)$$

ΔG_{gas}. The gas-phase energy profiles were explored using the Gaussian 98 program[23] at the Hartree–Fock (HF) level with the 6-31+G* basis set, unless stated otherwise. Each of the transition states was verified by a single imaginary frequency and an intrinsic reaction

(21) Strominger, J. L.; Ghuysen, J. M. *Science* **1967**, *156*, 213–221.
(22) Dudev, T.; Lim, C. *J. Am. Chem. Soc.* **1998**, *120*, 4450–4458.

Scheme 2. Schematic Diagram Showing the Inhibition of Penicillin-G by β-lactamase (E′)

Scheme 3. Schematic Diagram Showing the Inhibition of β-lactamase (E′) by Clavulanic Acid (Clav)
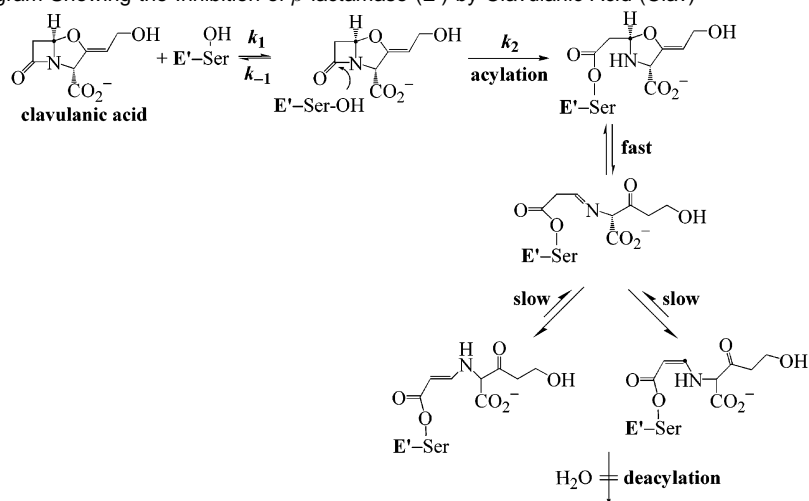
coordinate[24] calculation leading to the expected ground state and products. Furthermore, each of the intermediates was verified to be a local minimum on the potential energy surface by the absence of any imaginary frequencies. Using the fully optimized HF/6-31+G* geometries, the correlation energy was estimated with second-order Møller–Plesset (MP2) theory and the 6-31+G* basis set. The rate-limiting transition state of each reaction was reoptimized at the MP2/6-31+G* level, and the correlation energy was computed with larger basis sets.

To determine the thermodynamic parameters, vibrational frequencies were computed for the fully optimized structures of the stationary points along the reaction profile. The HF/6-31+G* frequencies were scaled by an empirical factor of 0.8929 to correct for any errors that may arise from anharmonicity in the potential energy surface, an inadequate basis set, and the neglect of electron correlation.[25] The zero-point energy (ZPE), thermal energy (E_T), and entropy (S) were calculated from the frequencies and geometries, according to standard statistical mechanical formulas.[26] The gas-phase free-energy barrier from A to B was calculated from the difference in the work term ΔPV, ΔE_{elec}, ΔZPE, ΔE_T, and ΔS at the temperature $T = 303.15$ K according to

$$\Delta G_{gas} = \Delta E_{elec} + \Delta \text{ZPE} + \Delta E_T - T\Delta S + \Delta PV \qquad (2)$$

ΔG_s. The solvation free energy, ΔG_s, was computed from the difference between the electrostatic potentials obtained by the numerical

solution to Poisson equation in the gas-phase ($\epsilon = 1$) and in aqueous solution ($\epsilon = 80$). The continuum dielectric calculations employed a $71 \times 71 \times 71$ lattice centered on the molecules with an initial spacing of 1.00 Å and refined with a spacing of 0.25 Å, ab initio geometries, and MP2/6-31+G* CHelpG[27] partial atomic charges. The low-dielectric region of the solute was assigned a dielectric constant of two to account for the electronic polarizability of the solute. This region was defined as the region inaccessible to contact by a 1.4-Å sphere rolling over a surface defined initially by CHARMM (version 22)[28] van der Waals radii.

The solute radii were then adjusted to reproduce the experimental hydration free energies of the model compounds listed in Table 1 because the experimental hydration free energies for the intact Peni and Clav molecules could not be found. Thus, the 1 positions of Clav and Peni were modeled by CH_3OCH_3 and CH_3SCH_3, respectively: the hydroxyethylidene group of Clav was modeled by $H_2C=CHCH_2OH$; the carboxyl group was modeled by $CH_3CO_2^-$; the carbonyl amide in the β-lactam ring was modeled by $CH_3CONHCH_3$; and the 1 positions of the Peni and Peni-db reaction products were modeled by CH_3SH. The atomic radii adjusted for both HF/6-31+G* and MP2/6-31+G* geometries and MP2/6-31+G* CHelpG[27] atomic charges reproduced the experimental free energies of the compounds to within 5% (Table 1).

Ring Strain Energy. We have developed an ab initio method for computing the strain energy of a ring molecule in our earlier work.[22] This method has been validated by reproducing the experimentally determined strain energies of mono- and bi-cyclohydrocarbons, cyclic

(23) Frisch, M. J.; Trucks, G. W.; Schlegel, H. B.; Scuseria, G. E.; Robb, M. A.; Cheeseman, J. R.; Zakrzewski, V. G.; Montgomery Jr., J. A.; Stratmann, R. E.; Burant, J. C.; Dapprich, S.; Millam, J. M.; Daniels, A. D.; Kudin, M. C.; Strain, K. N.; Farkas, O.; Tomasi, J.; Barone, V.; Cossi, M.; Cammi, R.; Mennucci, B.; Pomelli, C.; Adamo, C.; Clifford, S.; Ochterski, J.; Petersson, G. A.; Ayala, P. Y.; Cui, Q.; Morokuma, K.; Malick, D. K.; Rabuck, A. D.; Raghavachari, K.; Foresman, J. B.; Cioslowski, J.; Ortiz, J. V.; Stefanov, B. B.; Liu, G.; Liashenko, A.; Piskorz, P.; Komaromi, I.; Gomperts, R.; Martin, R. L.; Fox, D. J.; Keith, T.; Al-Laham, M. A.; Peng, C. Y.; Nanayakkara, A.; Gonzalez, C.; Challacombe, M.; Gill, P. M. W.; Johnson, B.; Chen, W.; Wong, M. W.; Andres, J. L.; Gonzalez, C.; Head-Gordon, M.; Replogle, E. S.; Pople, J. A. *Gaussian 98,* revision A.5; Gaussian, Inc.: Pittsburgh, PA, 1998.

(24) Gonzalez, C.; Schegel, H. B. *J. Phys. Chem.* **1990**, *94*, 5523−5527.
(25) Hehre, W. J.; Radom, L.; Schleyer, P. v. R.; Pople, J. A. *Ab Initio Molecular Orbital Theory*; John Wiley and Sons: New York, 1986.
(26) McQuarrie, D. A. *Statistical Mechanics*; Harper and Row: New York, 1976.
(27) Chirlian, L. E.; Francl, M. M. *J. Comput. Chem.* **1987**, *8*, 894−905.
(28) Brooks, B. R.; Bruccoleri, R. E.; Olafson, B. D.; States, D. J.; Swaminathan, S.; Karplus, M. *J. Comput. Chem.* **1983**, *4*, 187−217.

Table 1. Effective Solute Radii for Continuum Dielectric Calculations

model compounds	ΔG_s^{expt} (kcal/mol)	R_{eff}^a (Å)	$\Delta G_s^{calc,b}$ (kcal/mol)	$\Delta G_s^{calc,c}$ (kcal/mol)
CH_3OCH_3	-1.9^d	2.00 (C^{sp^3}) 1.77 (O^{ring}) 1.468 (H^C)	-1.84	-1.96
CH_3SCH_3	-1.5^d	2.00 (S)	-1.53	-1.45
CH_2CHCH_2OH	-5.0^d	1.875 (O) 1.75 (C^{sp^2}) 0.2245 (H^O)	-4.97	-5.13
$CH_3CO_2^-$	-77.0^e	1.60 (O)	-76.62	-76.65
$CH_3CONHCH_3$	-10.0^f	1.55 (N) 0.2245 (H^N)	-9.88	-10.23
CH_3SH	-1.2^d	2.55 (S^H)	-1.23	-1.18

^{a} Radius adjusted to reproduce the experimental hydration free energy of the model compound on the basis of its fully optimized HF/6-31+G* geometry and MP2/6-31+G* atomic charges. ^{b} Hydration free energy calculated using HF/6-31+G* geometry, MP2/6-31+G* charges, and radii in column 3. ^{c} Hydration free energy calculated using MP2/6-31+G* geometry, MP2/6-31+G* charges, and radii in column 3. ^{d} From Cramer & Truhlar, 1992.[44] ^{e} From Pearson, 1986.[45] ^{f} From Wolfenden, 1978.[46]

ethers, and amines. The ring-strain energy of an *n*-membered ring relative to an *r*-membered (reference) ring can be computed from

$$E_{RS} = E_n - E_r - (n - r)E_X \tag{3}$$

where X is the differential fragment, $-CH_2$, whose MP2/6-31+G*//HF/6-31+G* energy ($-39.167\ 153$ hartrees) was obtained as the difference between the energy of all-*trans*-hexane and that of all-*trans*-pentane.

The strain energy of an *n*-membered ring can also be computed relative to its acyclic counterpart containing the same number of heavy atoms. In this case, E_{RS} is given by

$$E_{RS} = E_{cyclo} - E_{acyclo} + E_{2H} \tag{4}$$

where E_{2H} accounts for the breaking of a C−C bond in the cyclic species and the addition of two more C−H bonds at both ends of the acyclic chain. The strain energies of the five-membered rings in Peni and Clav were computed relative to an acyclic molecule, which was derived by breaking the C2−C3 bond in Peni and Clav and adding a hydrogen atom each to C2 and C3. In the case of Peni, both C2 and C3 are sp^3 carbon atoms, thus the E_{2H} term was derived from ethane as follows:

$$E_{2H} = 2E_{C-H} - E_{C-C} \tag{5a}$$

where

$$E_{C-H} = E(CH_3-CH_3) - E(CH_3-CH_2^{\bullet}) \tag{5b}$$

and

$$E_{C-C} = E(CH_3-CH_3) - 2E(CH_3^{\bullet}) \tag{5c}$$

The MP2/6-31+G*//HF/6-31+G* E_{C-H} and E_{C-C} energies were computed to be equal to $-0.657\ 277$ and $-0.152\ 728$ hartrees, respectively, yielding $E_{2H} = -1.161\ 826$ hartrees. In the case of Clav, C2 is an sp^2 carbon, thus the E_{2H} term was computed from

$$E'_{2H} = E_{C-H} + E'_{C-H} - E'_{C-C} \tag{6a}$$

where

$$E'_{C-H} = E(CH_2{=}CH_2) - E(CH_2{=}CH^{\bullet}) \tag{6b}$$

$$E'_{C-C} = E(CH_2{=}CH-CH_3) - E(CH_2{=}CH^{\bullet}) - E(CH_3^{\bullet}) \tag{6c}$$

The MP2/6-31+G*//HF/6-31+G* E'_{C-H} and E'_{C-C} energies were

Table 2. Comparison of the Fully Optimized HF/6-31+G* and MP2/6-31+G* Geometry of Peni with the Respective Crystal Structure

	experiment^a	HF/6-31+G*	MP2/6-31+G*
	bond distance (Å)		
S1−C2	1.852	1.868	1.860
C2−C3	1.561	1.573	1.567
C3−N4	1.462	1.448	1.450
N4−C5	1.486	1.438	1.452
C5−S1	1.830	1.825	1.833
C5−C6	1.559	1.546	1.546
C6−C7	1.568	1.527	1.533
C7−N4	1.387	1.361	1.383
C7−O8	1.193	1.195	1.232
C3−C9	1.522	1.557	1.556
C2−C10	1.513	1.528	1.526
C2−C11	1.517	1.534	1.531
	bond angle (deg)		
C7−N4−C5	94.6	94.8	93.8
O8−C7−N4	131.7	133.1	132.7
C5−S1−C2	95.4	94.4	94.3
C5−N4−C3	117.0	117.8	117.1
S1−C2−C3	104.2	105.9	106.2
C6−C7−N4	91.7	91.9	91.8
S1−C5−N4	104.1	104.7	104.4
C2−C3−N4	105.2	105.2	104.8

^{a} From Gibon, V. et al. *Acta. Crystallogr., Sect. C* **1988**, *44*, 652.

computed to be equal to $-0.679\ 447$ and $-0.178\ 738$ hartrees, respectively. Using these values and the above E_{C-H} energy in eq 6a, $E'_{2H} = -1.157\ 986$ hartrees.

Results

Geometry Validation. To determine the accuracy of the HF/6-31+G* optimized geometries, we compared the fully optimized geometry of Peni (at both the HF/6-31+G* and MP2/6-31+G* levels) with the crystal structure of Peni from the Cambridge Structural Database. Table 2 shows that the HF/6-31+G* bond distances and angles are within ±0.05 Å and 1.7° of the respective X-ray values, with the largest discrepancy observed for the N4−C5 distance and the S1−C2−C3 angle. Including electron correlation improved the agreement with the experimental bond distances except for the C7−O8 bond length, which is overestimated by 0.04 Å. The close agreement between the experimental and HF/6-31+G* optimized geometries indicates that the HF/6-31+G* structures are adequate for mapping out the free-energy profiles presented in Figures 2−4.

Reaction 1: OH$^-$ + Peni. Scheme 4 shows the geometries of the major intermediates and transition states along the lowest gas-phase free-energy pathway for OH$^-$ attack at the carbonyl carbon of Peni. As the O(H)−C7 distance decreased, the hydroxide hydrogen rotated toward the Peni nitrogen, forming a transition state (TS-1A) at a O(H)−C7 distance of 2.06 Å and a tetrahedral intermediate (I-1A) at 1.44 Å. The I-1A intermediate underwent an endocyclic cleavage of the C7−N4 bond, accompanied by an intramolecular transfer of the hydroxyl proton to the amide nitrogen via TS-1B to yield I-1B. The subsequent C5−S1 cleavage of the five-membered thiazolidine ring via TS-1C yielded a ring-opened molecule (I-1C). However, the gas-phase free energy of I-1C was significantly higher than that of I-1B (by 13.0 kcal/mol) and slightly higher than that of the thiazolidine ring-opening transition state TS-1C (by 1.4 kcal/mol), indicating that it is unstable (Figure 2). (Several attempts to locate an intermediate with an energy lower than the TS-1C energy failed). Rotation about the C2−C3 bond via TS-1D

Scheme 4. Schematic Diagram Depicting Fully Optimized HF/6-31+G* Structures for the Reaction of OH⁻ with Peni. The number above each arrow is the *solution* free-energy difference between the molecule to the right of the arrow and the molecule to the left of the arrow
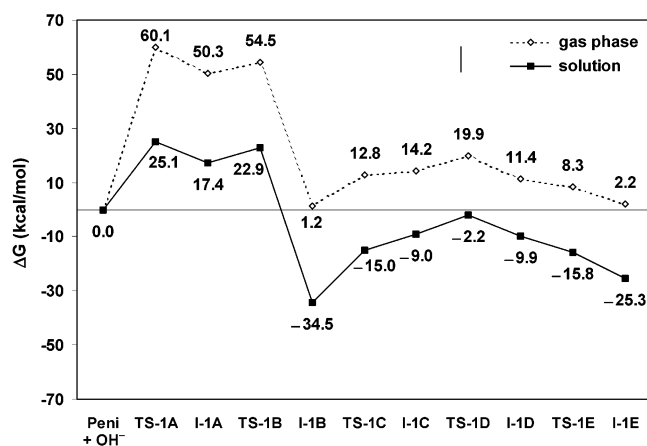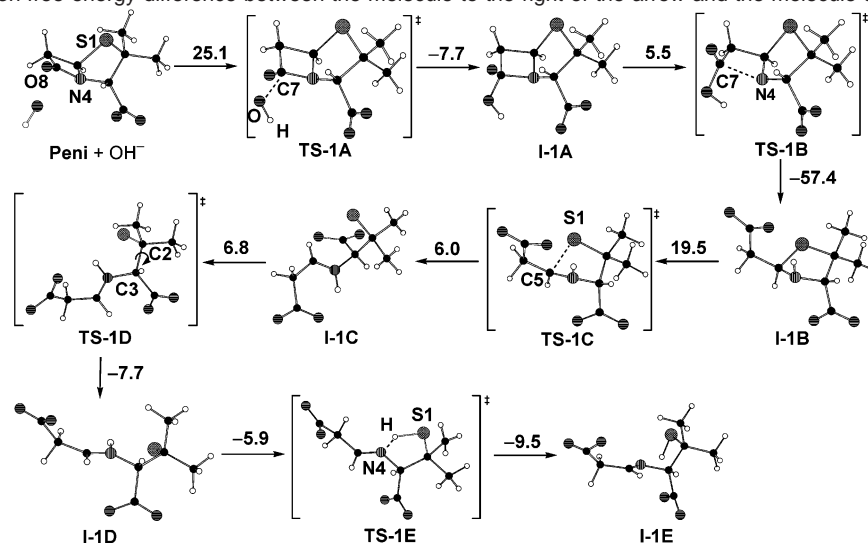
Figure 2. Relative MP2/6-31+G*//HF/6-31+G* activation free-energy profile for the gas-phase reaction of OH⁻ with Peni (dash line) and the change in profile upon solvation (solid line). The zero of energy corresponds to the reactants at infinite separation. The numbers correspond to the free energy of each stationary point along the *x*-axis relative to the reactants.

generated an intermediate (I-1D), where the amide proton could be transferred to S1 via TS-1E without an activation barrier. The resulting ring-opened product, I-1E, has a free energy similar to that of the five-membered ring I-1B molecule (Figure 2). The reaction of OH⁻ + Peni to yield I-1B or I-1E may not take place in the gas phase because the reaction free energy is slightly positive (1–2 kcal/mol, Figure 2).

Figure 2 shows how the gas-phase free-energy profile is changed upon solvation. The lowest free-energy pathway for the basic hydrolysis of Peni in solution was found to mimic that in the gas phase, except that thiazolidine ring-opening of I-1B yielded a less stable I-1E product. Because I-1B (−34.5 kcal/mol) has a more negative solution free energy than the ring-opened product, I-1E (−25.3 kcal/mol), and the infinitely separated reactants, the end-product of reaction 1 in *solution* is predicted to be the five-membered ring molecule, I-1B. As in the gas phase, the formation of the tetrahedral intermediate, I-1A, is rate-limiting in solution.

Reaction 2. OH⁻ + Clav. Comparison of the lowest gas-phase free-energy pathway for the OH⁻ + Clav reaction (Scheme 5 and Figure 3) with that for the OH⁻ + Peni reaction

(Scheme 4 and Figure 2) shows that the first two steps of reactions 1 and 2 are similar. In the first step, the nucleophile approached the carbonyl carbon of Clav, forming a transition state (TS-2A) at a O(H)−C7 distance of 2.09 Å and a tetrahedral intermediate (I-2A) at 1.45 Å (Scheme 4). In the second step, the I-2A intermediate underwent an endocyclic C7−N4 bond cleavage with a hydroxyl proton transfer to the amide nitrogen via TS-2B to yield I-2B. However, unlike the I-1B intermediate whose gas-phase free energy is positive (Figure 2), the I-2B intermediate has a substantial negative free energy (−10.5 kcal/mol, Figure 3) and underwent a C5−O1 cleavage of the five-membered oxazolidine ring via TS-2C to form a ring-opened intermediate (I-2C), which subsequently isomerized via TS-2D to an intermediate (I-2D) with a free energy (−10.0 kcal/mol, Figure 3) similar to that of the five-membered ring I-2B molecule. Finally, the N4 hydrogen of I-2D was transferred to O1 via TS-2E without an activation barrier to yield an enol product, I-2E, whose free energy (−18.9 kcal/mol) is almost twice as negative as the free energy of I-2B or I-2D. The enol product, I-2E, can undergo enol−keto tautomerization to yield a more stable keto form I-2F (−29.9 kcal/mol), which in turn can isomerize to form a less stable enamine I-2G (−25.6 kcal/mol) or I-2H (−21.3 kcal/mol) molecule (Scheme 5, Figure 3).

Figure 3 shows that the lowest free-energy pathway for the alkaline hydrolysis of Clav in solution is qualitatively similar to that in the gas phase, except that the enamine I-2H (−56.1 kcal/mol) is slightly more stable than I-2F (−54.6 kcal/mol) and I-2G (−53.7 kcal/mol). Unlike the case of the OH⁻ + Peni reaction, the product of reaction 2 in *solution* is predicted to be the ring-opened I-2F or I-2H rather than the five-membered ring molecule, I-2B (−38.7 kcal/mol). Furthermore, I-2F and I-2H are predicted to be more stable than the product of the OH⁻ + Peni reaction, I-1B (by 20.1 and 21.6 kcal/mol, respectively). As for the OH⁻ + Peni reaction, tetrahedral intermediate formation is rate-limiting in the gas phase and in solution, although the solution barrier (20.0 kcal/mol) is less than that for reaction 1 (25.1 kcal/mol).

Reaction 3: OH⁻ + Peni-db. Scheme 6 and Figure 4 show that the gas-phase and solution free-energy profiles for the alkaline hydrolysis of Peni-db differ from those for the alkaline

Scheme 5. Schematic Diagram Depicting Fully Optimized HF/6-31+G* Structures for the Reaction of OH⁻ with Clav. The number above each arrow is the *solution* free-energy difference between the molecule to the right of the arrow and the molecule to the left of the arrow
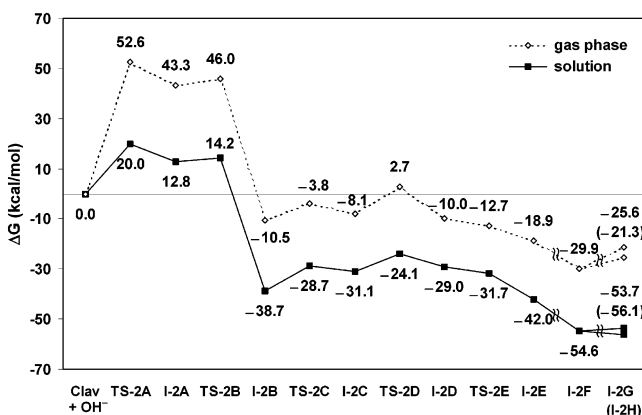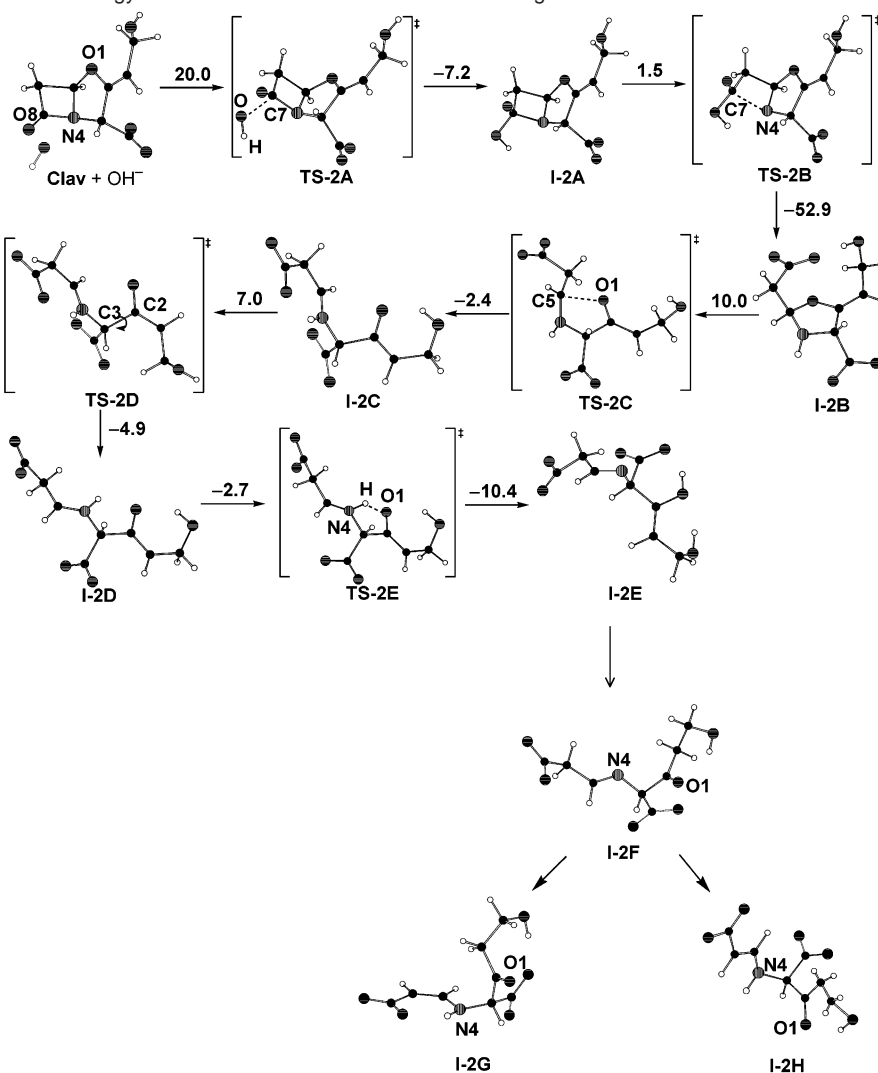
Figure 3. Relative MP2/6-31+G*//HF/6-31+G* activation free-energy profile for the gas-phase reaction of OH⁻ with Clav (dash line) and the change in profile upon solvation (solid line). The zero of energy corresponds to the reactants at infinite separation. The numbers correspond to the free energy of each stationary point along the *x*-axis relative to the reactants.

hydrolysis of Clav (Scheme 5 and Figure 3) but are similar to those for the alkaline hydrolysis of Peni (Scheme 4 and Figure 2). As for the OH⁻ + Peni reaction, a transition state (TS-3A) was formed at an O(H)−C7 distance of 2.09 Å followed by a tetrahedral intermediate (I-3A), which underwent intramolecular

C7−N4 bond cleavage and proton transfer via TS-3B to yield I-3B. Also, in analogy to reaction 1, the C5−S1 ring opening of the I-3B intermediate via TS-3C yielded a less stable I-3C molecule (Figure 4). Rotation about the C2−C3 bond via TS-3D to yield I-3D proceeded without an activation barrier. However, the subsequent transfer of the I-3D amide proton to S1 via TS-3E generated a less stable product (I-3E) with a slightly positive free energy 0.2 kcal/mol (Figure 4). Unlike the OH⁻ + Peni reaction where I-1B has a slightly positive gas-phase free energy (Figure 2), reaction 3 is predicted to yield I-3B as its gas-phase free energy is negative (−5.2 kcal/mol).

Figure 4 shows that the solution free-energy profile for the alkaline hydrolysis of Peni-db mimics the gas-phase profile in that the I-3B is more stable than the ring-opened molecules and the infinitely separated reactants. Therefore, it is predicted to be the end-product of reaction 3 in *solution*. As for reactions 1 and 2, the formation of the tetrahedral intermediate, I-3A, is rate-limiting in the gas phase and in solution. However, the solution free-energy barrier (21.7 kcal/mol) is less than that for reaction 1 (25.1 kcal/mol) but slightly greater than that for reaction 2 (20.0 kcal/mol).

Effect of Electron Correlation on the Rate-Limiting Transition States. Figures 2−4 show that, for the alkaline

Scheme 6. Schematic Diagram Depicting Fully Optimized HF/6-31+G* Structures for the Reaction of OH⁻ with Peni-db. The number above each arrow is the *solution* free-energy difference between the molecule to the right of the arrow and the molecule to the left of the arrow
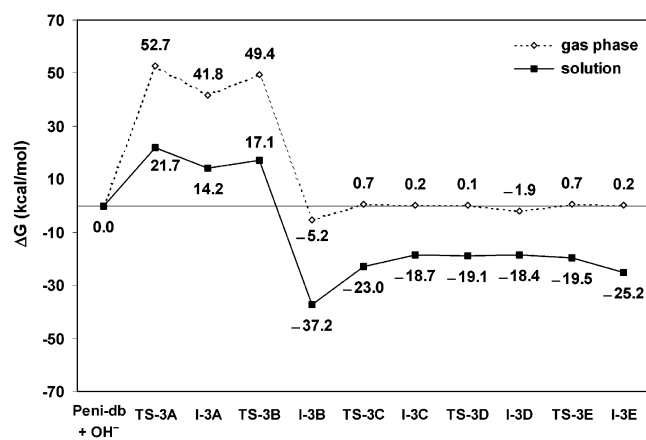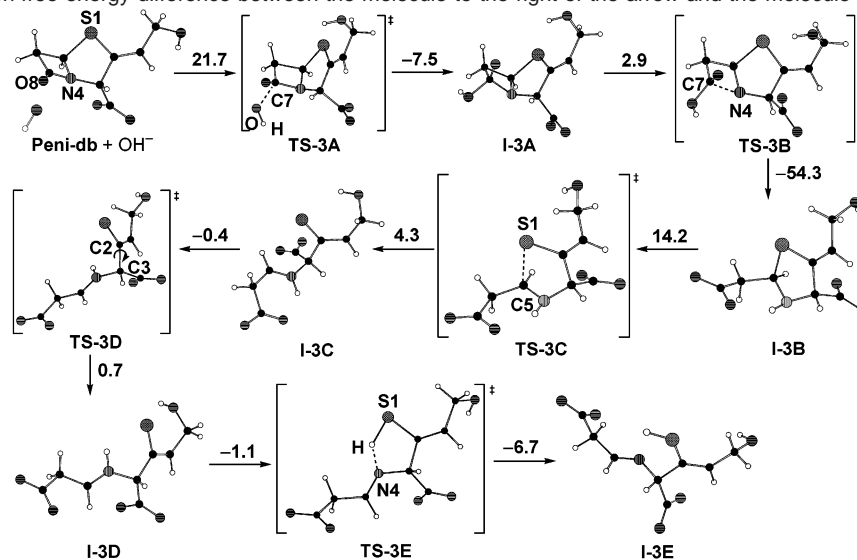
Figure 4. Relative MP2/6-31+G*//HF/6-31+G* activation free-energy profile for the gas-phase reaction of OH⁻ with Peni-db (dash line) and the change in profile upon solvation (solid line). The zero of energy corresponds to the reactants at infinite separation. The numbers correspond to the free energy of each stationary point along the x-axis relative to the reactants.

Table 3. Energy Dependence of the Rate-Limiting Transition States on Electron Correlation and Basis Set Size

theory level	MP2[a]	MP2[b]	MP2[b]	MP2[b]
basis set	6-31+G*	6-31+G*	6-31++G(2d,2p)	6-311++G(3df,3pd)
$\Delta E^{\ddagger}$(TS-1A)[c]	48.7	49.7	50.5	50.1
$\Delta E^{\ddagger}$(TS-2A)[c]	41.7	42.7	43.8	43.9
$\Delta E^{\ddagger}$(TS-3A)[c]	41.9	43.0	44.0	44.1

[a] Geometries optimized at the HF/6-31+G* level. [b] Geometries optimized at the MP2/6-31+G* level. [c] Energy relative to reactants separated at infinity.

Table 4. Relative Energies and Free Energies of the Rate-Limiting Transition States Located in the Gas Phase and in Solution at 303.15 K with Respect to Those of the Reactants Separated at Infinity in the Gas Phase[a]

reaction	O(H)–C7 (Å)	$\Delta E^{\ddagger b}$	$\Delta ZPE^{\ddagger}$	$\Delta E^{\ddagger}_T$	$T\Delta S^{\ddagger}$	$\Delta G^{\ddagger}_{gas}$	$\Delta G^{\ddagger}_{sln}$
Peni + OH⁻	2.27	50.1	1.2	0.7	−10.0	61.4	26.2
Clav + OH⁻	2.35	43.9	1.1	0.6	−9.8	54.9	22.9
Peni-db + OH⁻	2.34	44.1	1.0	0.6	−9.7	54.8	24.2

[a] All energies are reported to one decimal place in kcal/mol. [b] MP2/6-311++G(3df,3pd)//MP2/6-31+G* energy relative to those of the reactants separated at infinity in the gas phase.

hydrolyses of Peni, Clav, and Peni-db, the rate-limiting transition states are TS-1A, TS-2A, and TS-3A, located at a HF/6-31+G* O^H−C7 distance of 2.06, 2.09, and 2.09 Å, respectively. To include the effect of electron correlation in bond formation, these transition states were fully reoptimized at the MP2/6-31+G* level. Including electron correlation caused the earlier formation of the rate-limiting transition states,[29] as evidenced by a longer MP2/6-31+G* O^H−C7 distance of 2.27 Å for TS-1A, 2.35 Å for TS-2A, and 2.34 Å for TS-3A as compared to the corresponding HF/6-31+G* values. Using the MP2/6-31+G* optimized geometry, the gas-phase activation energy for each reaction was found to be greater than the respective MP2/6-31+G*//HF/6-31+G* value by about 1 kcal/mol (see Table 3).

To verify that the MP2/6-31+G*//MP2/6-31+G* activation energies are converged with respect to the basis set size, single-point energy calculations of the reactants and rate-limiting transition states were recomputed at the MP2 level using the MP2/6-31+G* optimized geometries with two larger basis sets. The results in Table 3 show that the MP2/6-31+G*, MP2/

6-31++G(2d,2p), and MP2/6-311++G(3df,3pd) energies of the rate-limiting transition states relative to the reactants differ by ≤1.2 kcal/mol. In particular, the MP2/6-31++G(2d,2p) and MP2/6-311++G(3df,3pd) activation energies agree to within 0.4 kcal/mol, suggesting that these values are converged with respect to the basis set size.

On the basis of the MP2/6-31+G* geometries and ChelpG charges, the solvation free energies of the reactants and rate-limiting transition states were computed and used together with the MP2/6-311++G(3df,3pd)//MP2/6-31+G* activation energies in eq 1 to compute the solution free-energy barriers. The resulting values for the alkaline hydrolyses of Peni, Clav, and Peni-db are 26.2, 22.9, and 24.2 kcal/mol, respectively (Table 4).

Strain Contribution of the Four-Membered β-Lactam Ring. To elucidate the ring strain of the β-lactam ring, we have computed the MP2/6-31+G*//HF/6-31+G* strain energies of various r-membered ring lactams (r = 4, 5, or 6) relative to

(29) Chang, N.-Y.; Lim, C. *J. Am. Chem. Soc.* **1998**, *120*, 2156−2167.

Table 5. MP2/6-31+G*//HF/6-31+G* Ring Strain Energies (kcal/mol) of Lactam Rings

	β-lactam	γ–lactam	δ–lactam
Reference molecule:			
	20.3[a]	−0.2[a]	0.9[a]
Reference molecule: γ-lactam	20.8[b]	0.0	0.1[b]

	Peni-4	γ–Peni-5	δ–Peni-6
Reference molecule:			
	14.5[a]	−8.1[a]	−5.8[a]
Reference molecule: γ–Peni-5	19.1[b]	0.0	2.4[b]

	Peni	γ–Peni	δ–Peni
Reference molecule:			
	18.8[a]	−1.9[a]	−0.6[a]
Reference molecule: γ–Peni	20.9[b]	0.0	1.1[b]

[a] Computed by eq 4. [b] Computed by eq 3.

their acyclic analogues in which the $-H_2C-CH_2-$ bond in the β-lactam ring is broken (see Methods). Table 5 shows that the strain energies are not linearly correlated with ring size: relative to the *acyclic* molecule the five-membered ring in γ-lactam, γ-Peni-5, or γ-Peni had less strain than the corresponding four-membered or six-membered ring. In fact, the ring strain energies of γ-lactam, γ-Peni-5, and γ-Peni relative to their *acyclic* counterparts are negative (−0.2, −8.1, and −1.9 kcal/mol). Hence, the five-membered γ-lactam ring can be considered to be strain-free. Consequently, the MP2/6-31+G*//HF/6-31+G* strain energies of the *r*-membered ring lactams in Table 5 were also computed relative to their five-membered ring analogues.
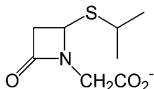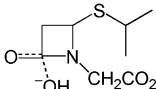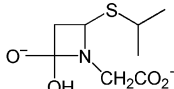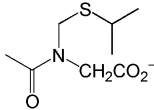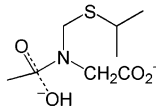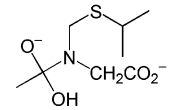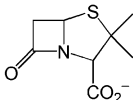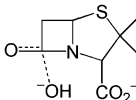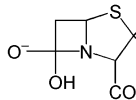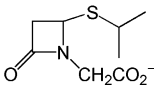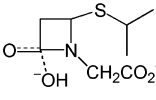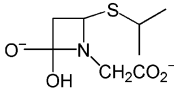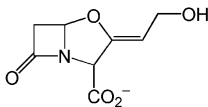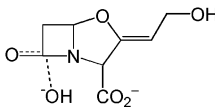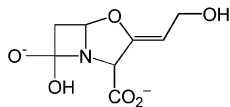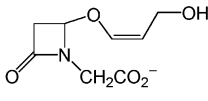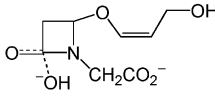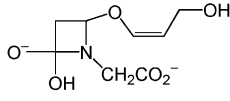
Table 5 shows that the strain energies of β-lactam, Peni-4, and Peni relative to their acyclic counterparts (20.3, 14.5, and

18.8 kcal/mol) or their five-membered analogues (20.8, 19.1, and 20.9 kcal/mol) are quite positive, implying that the four-membered ring is indeed strained, as predicted in previous works.[30] However, the four-membered ring strain does not appear to play a role in the tetrahedral intermediate formation, as evidenced by the lower strain energy of Peni-4 (14.5 kcal/mol) relative to that of the corresponding transition state (19.0 kcal/mol) or tetrahedral intermediate (17.9 kcal/mol) (see Table 6). In other words, ring strain is *not* relieved upon forming the four-membered ring transition state, Peni-4-TS, which has more ring strain than the ground-state molecule (by 4.5 kcal/mol).

(30) Page, M. I. *The Chemistry of β-lactams*; Chapman & Hall: London, 1992.

Table 6. MP2/6-31+G*//HF/6-31+G* Ring Strain Energies (kcal/mol) of the Ground States, Rate-Limiting Transition States, and Corresponding Intermediates Formed during the Alkaline Hydrolyses of Peni-4, Peni, and Clav

	Peni-4	Peni-4-TS	Peni-4-I
Reference Molecule:			
	14.5[a]	19.0[a]	17.9[a]

	Peni	TS-1A	I-1A
Reference Molecule:			
	5.6[a]	7.4[a]	0.7[a]
Reference Molecule: Peni	0.0	1.9	−4.8

	Clav	TS-2A	I-2A
Reference Molecule:			
	11.9[a]	15.1[a]	3.3[a]
Reference Molecule: Clav	0.0	3.2	−8.6

[a] Computed by eq 4.

Strain Contribution of the Five-Membered Ring in Peni and Clav. To elucidate this contribution in the alkaline hydrolyses of Peni and Clav, we have computed the MP2/6-31+G*//HF/6-31+G* strain energies of Peni and Clav, their rate-limiting transition states, and intermediates relative to the acyclic analogues in which the C2−C3 bond in the five-membered ring is broken. Table 6 shows that the five-membered rings are strained in Peni (5.6 kcal/mol) and Clav (11.9 kcal/mol), but are even more strained in the respective TS-1A (7.4 kcal/mol) and TS-2A (15.1 kcal/mol) transition states. The ring strain is almost relieved in the I-1A (0.7 kcal/mol) intermediate and to a large extent in I-2A (3.3 kcal/mol). Hence, the inherent strain of the five-membered ring does not appear to contribute to the reactivity of Peni or Clav.

Discussion

In the following, the findings of this work are first validated by a comparison to available experimental data such as the product distribution, rate-limiting step, and relative rates of Peni versus Clav alkaline hydrolysis. Note that the conclusions reached here are based on the *relative* free-energy changes as opposed to absolute free energies. By assessing how one or more substituents affect the free energy in the gas phase or in solution, it is the hope that systematic errors in the barriers of two similar reactions would cancel (see below).

Comparison with Experiment. A. Observed Products of Reaction 1. Figure 2 and Scheme 4 show that the thiazolidine ring of Peni prefers to remain closed than open, so the product of reaction 1 in *solution* is predicted to be the five-membered ring molecule, I-1B. This is consistent with the experimentally observed products of the alkaline hydrolysis of penicillin G, which is a mixture of *5R,6R*- and *5S,6R*-benzylpenicillolate (Figure 1).[31−33] Experimental studies of the alkaline hydrolysis of penicillin G showed that epimerization at C5 is pH-

(31) Bird, A. E.; Cutmore, E. A.; Jennings, K. R.; Marshall, A. C. *J. Pharm. Pharmacol.* **1983**, *35*, 138−143.

independent from pH 6 to pH 12.5, indicating that it occurs by a unimolecular ring opening of the five-membered thiazolidine ring to generate the iminium ion (equivalent to I-1C). However, no hydrolysis products of the iminium ion are observed, suggesting that S⁻ attacks the iminium ion to reclose the five-membered ring, forming C5−R or C5−S epimers.[30]

B. Observed Products of Reaction 2. Figure 3 and Scheme 5 show that, unlike the thiazolidine ring of Peni, which prefers to remain closed, the oxazolidine ring of Clav prefers to undergo C5−O1 cleavage to yield the ring-opened molecules, I-2F and I-2H, which are predicted to be much more stable than the end-product of the OH⁻ + Peni reaction, I-1B. This is consistent with experimental studies on the hydrolysis of Clav, showing that the end products are ring-opened molecules with both four- and five-membered rings destroyed. It is also consistent with experimental studies on the hydrolytic mechanism of Clav with β-lactamase,[17−19] suggesting that the oxazolidine ring opens and is trapped in the open position by ketonization of the enolate formed to yield the imine (equivalent to I-2F), which subsequently transfers a methylene hydrogen to yield an enamine (equivalent to I-2G) that may isomerize to the more stable *trans* form (equivalent to I-2H). Hence, the initial acyl-enzyme intermediate (equivalent to I-2B) is converted to a chemically inert vinylogous carbamate (equivalent to I-2G or I-2H) that transiently inhibits the β-lactamase enzyme.[20]

C. Rate-Limiting Step. Figures 2-4 show that tetrahedral intermediate formation, rather than the opening of the four-membered β-lactam ring or the five-membered thiazolidine/oxazolidine ring, is rate-limiting in the alkaline hydrolysis of β-lactam molecules Peni, Clav, or Peni-db. These predictions are consistent with experiments showing a first-order dependence on hydroxide ion concentration and a negative Brönsted value for the rates of alkaline hydrolysis of β-lactams, indicating rate-limiting tetrahedral intermediate formation.[30,34,47]

D. Relative Reaction Rates. The alkaline hydrolysis of Peni is predicted to be slower than that of Clav, as evidenced by a larger activation free energy for the former as compared to the latter (26.2 vs 22.9 kcal/mol, Table 4). Furthermore, the activation free-energy difference, $\Delta G^{\ddagger}_{sln}(Peni) - \Delta G^{\ddagger}_{sln}(Clav)$, of 3.3 kcal/mol is in quantitative accord with the experimental estimate of 3.5 kcal/mol derived from the second-order rate constants measured at 303.15 K for the alkaline hydrolyses of Peni (7.4×10^{-3} dm³ mol⁻¹ s⁻¹) and Clav (2.39 dm³ mol⁻¹ s⁻¹).[30] The close agreement with experimental findings probably reflects the cancellation of systematic errors in the computed (a) gas-phase activation free energies for the two reactions and (b) solvation free energies of Peni and Clav as well as the corresponding rate-limiting transition states.

Comparison with Previous Calculations. Several theoretical studies on parts of the hydrolyses of β-lactam-containing compounds have been carried out.[35,36,47−49] In particular, the basic hydrolyses of a series of β-lactam molecules including Clav and penicillin G have been studied using semiempirical methods.[35,36] These studies assumed that, in the *gas* phase, the approach of OH⁻ to the Clav anion occurred spontaneously without an energy barrier to form a tetrahedral intermediate that was more stable than the reactants. In particular, Frau et al.[35] found that the breakdown of the four-membered β-lactam ring was rate-limiting in the gas-phase alkaline hydrolysis of Clav. These findings are at odds with the present ab initio calculations showing that tetrahedral intermediate formation rather than β-lactam ring-opening is rate-limiting in the gas-phase basic hydrolysis of β-lactam molecules such as Peni and Clav (see Figures 2 and 3). The finding that the dianionic tetrahedral intermediate is formed without any energy barrier in the gas phase seems unlikely, as the approach of two negatively charged molecules, OH⁻ and Clav⁻, would be expected to induce a barrier. However, if the β-lactam molecule was *neutral*, for example, by protonating the carboxyl group,[37] both experimental[38] and theoretical[39−42] studies support a barrierless, exothermic formation of the tetrahedral intermediate in the gas phase.

Factors Governing the Observed Products. A. Contribution from Position 1. This can be assessed by comparing the solution free-energy profiles for the alkaline hydrolyses of Peni-db (Figure 4) and Clav (Figure 3), which differ only at position 1. C5−S1 cleavage of the thiazolidine ring of Peni-db led to less stable products, whereas C5−O1 cleavage of the oxazolidine ring of Clav yielded more stable products. Replacing S1 by an oxygen facilitates the cleavage of the second fused ring, as evidenced by a lower I-2B → TS-2C barrier (10.0 kcal/mol, Scheme 5) compared to the corresponding I-3B → TS-3C barrier (14.2 kcal/mol, Scheme 6). Furthermore, the O1 atom in Clav can abstract a proton easier than the less polar S1 atom to yield thermodynamically more stable products, as evidenced by the more negative solution free energies of TS-2E (−31.7 kcal/mol) and I-2E (−42.0 kcal/mol) relative to TS-3E (−19.5 kcal/mol) and I-3E (−25.2 kcal/mol).

B. Contribution from Position 2. This can be assessed by comparing the solution free-energy profiles for the alkaline hydrolyses of Peni-db (Figure 4) and Peni (Figure 2), which differ only at position 2. Replacing two methyl groups in Peni with a hydroxyethylidene group reduced the C5−S1 cleavage barrier (from 19.5 to 14.2 kcal/mol) and eliminated the rotational barrier about the C2−C3 bond (from 6.8 to −0.4 kcal/mol, compare Schemes 4 and 6). However, the latter effect may not be significant in nonalkaline solutions or in the enzyme, where intermolecular (as opposed to intramolecular) proton transfer to the S1 atom could occur via water molecules or nearby active site residues, thus eliminating the need for C2−C3 rotation.

To elucidate why the O1 atom and the hydroxyethylidene group in Clav substantially reduces the barrier for five-membered ring opening, we compared the charge distributions of the ring-opening TS-C transition states and the respective I-B intermediates. ChelpG[27] and Merz−Kollman[50,51] charges were calculated at the MP2/6-31+G* level to verify that the

(32) Kessler, D. P.; Cushman, M.; Ghebre-Sellassie, I.; Knevel, A. M.; Hem, S. L. *J. Chem. Soc., Perkin Trans. 2* **1983**, 1699.
(33) Davis, A. M.; Page, M. I. *J. Chem. Soc., Chem. Commun.* **1985**, 1702−1704.
(34) Proctor, P.; Genmantel, N. P.; Page, M. I. *J. Chem. Soc., Perkin Trans. 2* **1982**, 1185.
(35) Frau, J.; Donoso, J.; Muñoz, F.; García Blanco, F. *Helv. Chim. Acta* **1994**, *77*, 1557−1569.
(36) Frau, J.; Donoso, J.; Muñoz, F.; García Blanco, F. *THEOCHEM* **1997**, *390*, 255−263.
(37) Bounaim, L.; Smeyers, N. J.; Gonzalez-Jonte, R. H.; Alvarez-Idaboy, J. R.; Ezzamarty, A.; Smeyers, Y. G. *THEOCHEM* **2001**, *539*, 233−243.
(38) Olmstead, W. N.; Brauman, J. I. *J. Am. Chem. Soc.* **1977**, *99*, 4219−4228.
(39) Petrolongo, C.; Ranghino, G.; Scordamaglia, R. *Chem. Phys.* **1980**, *45*, 279.
(40) Weiner, S. J.; Singh, U. C.; Kollman, P. A. *J. Am. Chem. Soc.* **1985**, *107*, 2219−2229.
(41) Madura, J. D.; Jorgensen, W. L. *J. Am. Chem. Soc.* **1986**, *108*, 2517−2527.
(42) Frau, J.; Donoso, J.; Muñoz, F.; Blanco García, F. *J. Comput. Chem.* **1992**, *13*, 681−692.

Table 7. Contributions to the Rate Acceleration of Clav Relative to Peni and Peni-db as well as Those of Peni-db Relative to Peni[a]

	Clav − Peni	Clav − Peni-db	Peni-db − Peni
$\Delta\Delta E^{\ddagger}_{gas}$[b]	−6.2	−0.2	−6.0
$\Delta\Delta E^{\ddagger}_{T}$[b]	−0.1	0.0	−0.1
$\Delta(T\Delta S^{\ddagger})$[b]	0.2	−0.1	0.3
$\Delta\Delta G^{\ddagger}_{gas}$[b]	−6.5	0.1	−6.6
$\Delta\Delta G_{s}(TS)$[c]	−1.0	−4.4	3.4
$\Delta\Delta G_{s}(GS)$[d]	−4.2	−3.1	−1.1
$\Delta\Delta G^{\ddagger}_{sln}$[b,e]	−3.3	−1.3	−2.0

[a] All energies are reported to one decimal place in kcal/mol. [b] Ground-state reactants to the rate-limiting transition state. [c] Difference between the solvation free energies of the rate-limiting transition states. [d] Difference between the solvation free energies of the ground states. [e] $\Delta\Delta G^{\ddagger}_{sln} = \Delta\Delta G^{\ddagger}_{gas} + \Delta\Delta G_{s}(TS) - \Delta\Delta G_{s}(GS)$.

trends obtained do not change with the method used to determine the charges. The negative charge on the atom at position 1 increased by −0.16e (ChelpG or Merz−Kollman) in going from I-1B to TS-1C. However, this increase is reduced by 0.04e (ChelpG) or 0.03e (Merz−Kollman) when the two methyl groups at position 2 were replaced with a hydroxyethylidene group. In analogy, the negative charge increase for atom 1 in going from I-3B to TS-3C (−0.13 to −0.12 e) is reduced by 0.06e (ChelpG) or 0.04e (Merz−Kollman) when S1 is replaced by an oxygen. Hence, the net effect of O1 and the hydroxy-ethylidene group in Clav is to reduce the increase in negative charge on the departing atom in the five-membered ring-opening transition state.

Factors Governing the Enhanced Reactivity of Clav Relative to Peni. The rate-limiting step in the alkaline hydrolyses of Peni and Clav is the nucleophilic addition of a negative hydroxide ion to the carbonyl carbon of a deprotonated acid. Thus, it is not surprising that solute−solute (as opposed to solute−solvent) electrostatic interactions govern the enhanced reactivity of Clav relative to Peni, as evidenced by the dominant gas-phase activation energy difference, $\Delta\Delta E^{\ddagger}_{gas}$ (−6.2 kcal/mol, see Table 7). Gas-phase vibrational energies and entropies make negligible contributions to the rate acceleration ($\Delta\Delta E^{\ddagger}_{T} = -0.1$ kcal/mol and $\Delta(T\Delta S^{\ddagger}) = 0.2$ kcal/mol, Table 7). Although the solvation free energies of both Clav (−67.9 kcal/mol) and its corresponding rate-limiting TS-2A (−193.2 kcal/mol) transition state are more favorable than those of Peni (−63.5 kcal/mol) and TS-1A (−191.2 kcal/mol), respectively, the differential solvation of the transition states makes a negative contribution (−1.0 kcal/mol) to $\Delta\Delta G^{\ddagger}_{sln}$, whereas the differential solvation of the ground states makes a positive contribution (4.2 kcal/mol) to $\Delta\Delta G^{\ddagger}_{sln}$. The net effect of solvation is to offset the favorable gas-phase $\Delta\Delta G^{\ddagger}_{gas}$ contribution to the rate accelera-tion. This is in contrast to the case of the hydrolyses of phosphate esters, in which solvent effects have been found to contribute significantly to the enhanced rate of the alkaline hydrolysis of a five-membered ring phosphate relative to its acyclic or six-membered ring counterpart.[29,43]

A. Contribution from Position 1. This can be assessed by comparing the contributions to the alkaline hydrolysis rate of Clav with those of Peni-db. Table 7 shows that replacing the S1 atom in Peni-db with an oxygen in Clav does not seem to enhance the reactivity of OH⁻ toward Clav in the gas phase, as evidenced by the negligible $\Delta\Delta E^{\ddagger}_{gas}$ (−0.2 kcal/mol) and $\Delta\Delta G^{\ddagger}_{gas}$ (0.1 kcal/mol) values. In aqueous solution, the presence of a more polar oxygen in the five-membered ring causes Clav to be better solvated than Peni-db by −3.1 kcal/mol, and the

rate-limiting transition state TS-2A to be better solvated than TS-3A by −4.4 kcal/mol. Consequently, replacing a sulfur with an oxygen at position 1 makes a small contribution (−1.3 kcal/mol) to the observed rate acceleration of Clav relative to Peni alkaline hydrolysis because of the greater solvent stabilization of the oxygen-containing TS-2A transition state relative to its sulfur-containing TS-3A counterpart.

B. Contribution from Position 2. This can be assessed by comparing the contributions to the alkaline hydrolysis rate of Peni-db with those of Peni. Table 7 shows that the *gas-phase* contributions to the alkaline hydrolysis rate of Peni-db relative to Peni are similar to those of Clav relative to Peni. However, the solvation free-energy difference between the rate-limiting transition states, $\Delta G_{s}(TS-3A) - \Delta G_{s}(TS-1A)$, is positive, implying a less favorable solvation of the transition state when the two methyl groups at position 2 are replaced by a hydroxyethylidene group. These results in conjunction with those of Clav relative to Peni-db suggest that the enhanced reactivity of Clav relative to Peni is due mainly to the substitution of two methyl groups with a hydroxyethylidene group at position 2 and, to a lesser extent, the exchange of a sulfur atom for an oxygen atom at position 1.

To elucidate why replacing two methyl groups with a hydroxyethylidene group lowered the gas-phase energy barrier of Peni-db relative to Peni, we compared the MP2/6-31+G* ChelpG[27] charge distributions of Peni, Clav, and Peni-db and the corresponding rate-limiting transition states. Replacing two methyl groups in Peni with a hydroxyethylidene group in Peni-db increased the positive charge on the carbonyl C7 atom by only 0.03e (ChelpG). However, the same substitution in the TS-3A transition state increased the positive charge on the carbonyl C7 atom relative to that in TS-1A by 0.14e. If the substitution was made at position 1 instead of position 2, with the S1 atom in TS-3A replaced by an oxygen in TS-2A, the positive charge on the carbonyl C7 atom remained the same. This suggests that the hydroxyethylidene group at position 2 may stabilize TS-3A relative to TS-1A through more favorable electrostatic interactions between the incoming hydroxide anion and the positively charged C7 atom. The computed Merz−Kollman[50,51] charges also show the same trend as the ChelpG ones except that replacing two methyl groups with a hydroxyethylidene group resulted in an increase of the C7 positive charge not only in the transition state (by 0.09e) but in the ground state as well (by 0.08e), suggesting that the hydroxyethylidene group may enhance the nucleophilic addition of OH⁻ to the C7 atom in Clav relative to Peni.

Ring Strain Contribution. It has been suggested that the activity of penicillin is due to the inherent strain of the four-membered β-lactam ring.[21] The ring strain energies in Table 6 (Peni-4 series) show that, in alkaline hydrolyses, the inherent

(43) Dejaegere, A.; Liang, X.; Karplus, M. *J. Chem. Soc., Faraday Trans.* **1994**, *90*, 1763−1770.
(44) Cramer, C. J.; Truhlar, D. G. *J. Comput.-Aided Mol. Des.* **1992**, *6*, 629−666.
(45) Pearson, R. G. *J. Am. Chem. Soc.* **1986**, *108*, 6109−6114.
(46) Wolfenden, R. *Biochemistry* **1978**, *17*, 201.
(47) Massova, I.; Kollman, P. A. *J. Phys. Chem. B* **1999**, *103*, 8628−8638.
(48) Coll, M.; Frau, J.; Vilanova, B.; Donoso, J.; Muñoz, F.; García Blanco, F. *J. Phys. Chem. A* **1999**, *103*, 8879−8884.
(49) Diaz, N.; Suarez, D.; Sordo, T. L.; Merz, K. M., Jr. *J. Phys. Chem. B* **2001**, *105*, 11302−11313.
(50) Singh, U. C.; Kollman, P. A. *J. Comput. Chem.* **1984**, *5*, 129.
(51) Besler, B. H.; Merz, K. M., Jr.; Kollman, P. A. *J. Comput. Chem.* **1990**, *11*, 431.

strain of the four-membered β-lactam ring is not relieved in the Peni-4-TS transition state or in the corresponding tetrahedral intermediate, whose four-membered ring remains intact. Therefore, β-lactam ring strain does not seem to facilitate the alkaline hydrolyses of β-lactam molecules such as Peni or Clav, consistent with the finding that the rate-limiting step is the formation of the tetrahedral intermediate rather than the breakdown of the β-lactam ring.[30] It is also consistent with the observation that the reaction rate[30] involving the β-lactam molecule in Table 5 (6.1×10^{-5} dm^3 mol^{-1} s^{-1}) is only 3 times greater than that of its acyclic counterpart (2.3×10^{-5} dm^3 mol^{-1} s^{-1}), but the rate acceleration due to the relief of the four-membered ring strain (20.3 kcal/mol relative to an acyclic analogue, Table 5) should be much greater (up to 10^{15} times instead of 3). Furthermore the I-1A molecule in Table 6 is nearly strain-free, thus ring strain does not facilitate the opening of its four-membered β-lactam ring.

The ring strain energies in Table 6 (Peni and Clav series) also show that the increase in the five-membered ring strain in going from Clav to its rate-limiting transition state (3.2 kcal/mol) is larger than that in going from Peni to its rate-limiting transition state (1.9 kcal/mol). Hence, the five-membered oxazolidine ring strain does not play a role in the observed rate acceleration of the alkaline hydrolysis of Clav relative to Peni.

Conclusions

The calculations have revealed the reaction mechanisms for the alkaline hydrolyses of Peni, Clav, and Peni-db. All three reactions share a common two-step mechanism of opening the four-membered β-lactam ring, which involves hydroxide ion attack at the carbonyl carbon of the β-lactam ring to form a tetrahedral intermediate, followed by the C7–N4 cleavage of the β-lactam ring with a concurrent intramolecular transfer of the hydroxide proton to the amide nitrogen. However, the subsequent C5–S1 cleavage of the five-membered thiazolidine ring of Peni or Peni-db yields less stable products, whereas the C5–O1 cleavage of the oxazolidine ring of Clav generates more stable products. The rate-limiting step in the alkaline hydrolysis of Peni, Clav, or Peni-db is the formation of the transition state (TS-1A, TS-2A, or TS-3A) that leads to the tetrahedral intermediate rather than the opening of the four-membered β-lactam ring or the five-membered thiazolidine/oxazolidine ring.

The different natures and stabilities of the products found in the alkaline hydrolyses of Peni and Clav are governed by the oxygen atom at position 1 as well as the hydroxyethylidene group at position 2 in Clav, which lower the ring-opening barrier of the five-membered ring. In addition, the O1 atom of Clav can abstract a proton easier than the less polar S1 of Peni. Consequently, after the opening of the four-membered β-lactam ring, C5–O1 cleavage of the five-membered oxazolidine ring of I-2B yields a more stable ring-opened I-2E molecule that can isomerize to an even more stable enamine I-2H molecule.

The enhanced reactivity of Clav relative to Peni is governed primarily by the hydroxyethylidene group and, to a lesser extent, the O1 atom in Clav. Replacing two methyl groups at position 2 with a hydroxyethylidene group results in an increase in the positive charge on the carbonyl C7 atom, therefore enhancing favorable electrostatic interactions with the incoming hydroxide anion. Replacing a sulfur at position 1 with an oxygen causes

a greater solvent stabilization of the oxygen-containing transition state as compared to the respective ground state. The five-membered oxazolidine ring strain of Clav is found *not* to play a role in the enhanced rate of the alkaline hydrolysis of Clav relative to Peni. The inherent strain of the four-membered β-lactam ring or five-membered ring was found *not* to accelerate the alkaline hydrolyses of β-lactam molecules such as Peni or Clav. This is consistent with the observation that the rate-limiting step does not involve the breakdown of the four-membered β-lactam ring or five-membered thiazolidine/oxazolidine ring.

The above results suggest that one of the reasons why Clav can inhibit β-lactamase while penicillin G cannot is because its hydroxyethylidene group at position 2 could facilitate the nucleophilic addition of the active site serine but not the two methyl groups in penicillin G. Furthermore, its hydroxyethylidene group and O1 atom could facilitate the opening of the five-membered ring and in addition, the O1 atom could abstract a proton easier than the less polar S1 in penicillin G, leading to relatively inert enzyme intermediates. Thus, the substituents at positions 1 and 2 allow Clav to react with β-lactamase faster than penicillin G, forming a hydrolytically stable acyl-enzyme, therefore freeing penicillin G to block the active site of transpeptidase.

The above results show how calculations can provide new insight into the reactivity differences between two commonly used antibiotics, Peni and Clav. In general, the approach presented in this work, using fictitous hybrid molecules such as Peni-db, ab initio electronic structure calculations combined with continuum dielectric methods, as well as the validation steps and analyses described herein, can be applied to other biologically active compounds or substrates. The results of such calculations could provide new insights into the *intrinsic* chemical reactivity differences between similar substrates by identifying the relative contributions of individual substituents (including ring strain for ring molecules) to the different reaction rates of the molecules. In this way, the effects of substituents on enzyme recognition/function can be isolated from their effects on *intrinsic* chemical reactivity. This work also shows that the relative kinetic reactivities and thermodynamic stabilities of *designed* biologically active compounds such as β-lactam antibiotics could be reliably predicted before carrying out experiments, thus potentially saving time and money.

Supporting Information Available: Tables listing electronic energies, zero-point energies, thermal energies, entropies, gas-phase free energies, solvation free energies, and solution free energies relative to those of the reactants separated at infinity. This material is available free of charge via the Internet at http://pubs.acs.org.

JA020788G